

Clonal Interference, Multiple Mutations, and Adaptation in Large Asexual Populations

Craig A. Fogle*, James L. Nagle*, and Michael M. Desai†

**Department of Physics, University of Colorado at Boulder, Boulder CO 80305*

†Lewis-Sigler Institute for Integrative Genomics, Princeton University, Princeton NJ 08544

(Dated: April 6, 2008)

Abstract

Two important problems affect the ability of asexual populations to accumulate beneficial mutations, and hence to adapt. First, clonal interference causes some beneficial mutations to be outcompeted by more-fit mutations which occur in the same genetic background. Second, multiple mutations occur in some individuals, so even mutations of large effect can be outcompeted unless they occur in a good genetic background which contains other beneficial mutations. In this paper, we use a Monte Carlo simulation to study how these two factors influence the adaptation of asexual populations. We find that the results depend qualitatively on the shape of the distribution of the effects of possible beneficial mutations. When this distribution falls off slower than exponentially, clonal interference alone reasonably describes which mutations dominate the adaptation, although it gives a misleading picture of the evolutionary dynamics. When the distribution falls off faster than exponentially, an analysis based on multiple mutations is more appropriate. Using our simulations, we are able to explore the limits of validity of both of these approaches, and we explore the complex dynamics in the regimes where neither are fully applicable.

INTRODUCTION

The accumulation of beneficial mutations drives adaptation and evolutionary innovation. Yet despite its central importance, the evolutionary dynamics by which a population accumulates such mutations is poorly understood. To better understand adaptation in any particular system, we must ask two questions. First, what is the range of beneficial mutations that are possible given the particular environmental challenge and genetic state of the population? Second, given this set of possibilities, what will actually happen probabilistically?

The first of these questions is fundamentally empirical, though Orr and Gillespie have argued on general theoretical grounds that the distribution of fitness effects of beneficial mutations should be exponential (GILLESPIE, 1983, 1984, 1991; ORR, 2002, 2003). A variety of recent experimental studies are roughly consistent with this exponential expectation (DEPRISTO *et al.*, 2005; IMHOF and SCHLOTTERER, 2001; KASSEN and BATAILLON, 2006; LUNZER *et al.*, 2005; ROKYTA *et al.*, 2005; ROZEN *et al.*, 2002; SANJUAN *et al.*, 2004). However, beneficial mutations are rare and their fitness effects are difficult to measure precisely, so these experimental studies are generally based on relatively few total mutations and have correspondingly limited resolution. The tail of the distribution, which refers to the rare mutations which confer a very large fitness benefit, is particularly hard to measure. Further, the spectrum of beneficial mutations available to a population is likely to vary with genetic background, history, and the environment, so it is unclear how far we can generalize from individual experimental studies. Thus it is still unknown whether in general the distribution of mutant effects, particularly of large-effect mutations, is exponential.

Even if we knew the precise distribution of mutational possibilities, it is not clear how a population would evolve. Because mutations are random events, there will inevitably be some randomness in how a given population adapts. What we would like to understand is the statistics of which beneficial mutations are more or less likely to contribute to adaptation, and the dynamics by which they do so. That is, given a set of things that are possible, what is the probability that any given one of them will actually occur and contribute to the adaptation of the population? What is the evolutionary dynamics by which they do so? In this paper, we focus on how the distribution of mutations that actually occur and spread

through the entire population (i.e. fix), $\rho_f(s)$, depends on the distribution of mutations that are possible, $\rho(s)$, where s is the fitness benefit from a single mutation. We explore these features as a function of the population size N and the overall mutation rate U . Besides its importance in understanding adaptation, this question is relevant in practical attempts to measure the distribution of possible mutations, since $\rho_f(s)$ is much easier to measure experimentally than $\rho(s)$. We also examine some aspects of the dynamics by which the mutations that fix do so.

There are a number of effects that make the distribution of mutations that fix different from the distribution of all possible mutations. First, most beneficial mutations that occur are lost rapidly by random genetic drift. If a beneficial mutation is particularly lucky, it will avoid this stochastic loss and reach a high enough frequency that thereafter its dynamics become dominated by selection rather than drift. We refer to this process as the *establishment* of the beneficial mutation. Mutations of larger effect are more likely to survive random drift — they have a higher establishment probability — so this will tend to bias the distribution of mutations that actually fix towards larger-effect mutations, relative to the distribution of mutations that are possible (HALDANE, 1927; ROZEN *et al.*, 2002).

Once a mutation has become established, it will fix provided that nothing else interferes. However, this fixation takes time, and other beneficial mutations can become established in individuals without the original mutation before the original mutation can fix. In an asexual population, if one or more of these other mutations has a larger fitness benefit than the original mutation, the original mutation will eventually be out-competed and driven to extinction. This process is known as *clonal interference* (GERRISH, 2001; GERRISH and LENSKI, 1998; WILKE, 2004). The same process also operates in a sexual population, where it is referred to as the Hill-Robertson effect, but is mitigated because the two competing mutations can potentially recombine onto the same genome and fix together (HILL and ROBERTSON, 1966). In this paper, we focus exclusively on asexual populations, where this effect is strongest.

In a small population with a small to modest mutation rate, the establishment of a beneficial mutation is an extremely rare event. Thus clonal interference is unlikely to occur, and the distribution of mutations that fix is simply the distribution of mutations that establish. In a larger population, or one with a higher mutation rate, however, clonal interference can be extremely common. Because small-effect mutations are more likely to be interfered with

than large-effect mutations, clonal interference biases the distribution of mutations that fix towards those of large effect. This bias has been analyzed in detail both theoretically (GERRISH and LENSKI, 1998; WILKE, 2004) and experimentally (DE VISSER *et al.*, 1999; DE VISSER and ROZEN, 2005).

These analyses of clonal interference only consider mutations which occur in the wild-type population; they assume that the largest such mutation is the one that fixes. The possibility of double mutations in a single organism is neglected. But, in fact, even if a more-fit mutation B occurs before an earlier but less-fit mutation A fixes, A may still survive, because an individual with mutation A can get another mutation C such that the A-C double mutant is more fit than B. Recently, DESAI and FISHER (2007) showed that whenever clonal interference is important, these multiple mutations are also at least of comparable importance — and, in fact, many large asexual populations will often routinely have triple or quadruple mutations (DESAI *et al.*, 2007). Because small-effect mutations are more common than mutations of larger effect, they are more likely to form double mutants. Thus the possibility of multiple mutations biases the distribution of mutations that fix back towards those of smaller effect. In short, it will often be the case that getting two small-effect mutations is more common than getting a single (rarer) large-effect mutation. This effect depends on the shape of the distribution of mutational effects: the rarer large-effect mutations are compared to small-effect ones, the stronger the multiple-mutation effect should be. The importance of this effect also depends on population size and mutation rate, though in a somewhat different way than clonal interference does.

In addition to affecting the distribution of mutations that fix, multiple mutations also have an important impact on the evolutionary dynamics. Different individuals have different numbers and strengths of beneficial mutations, so a large population can maintain substantial variation in fitness. It is only those mutations that occur in the most-fit individuals which have the best chance of surviving and contributing to the long-term adaptation of the population. Thus the dynamics of adaptation are slowed down, limited by the rate at which good mutations occur in good backgrounds.

Because the distribution of beneficial mutations which fix depends in a subtle way on both clonal interference and multiple-mutation effects, it cannot be fully understood without a complete model which includes both. No analytical results from such a model yet exist,

though KIM and ORR (2005) have analyzed a model which includes some aspects of both effects. In this paper, we address this question using Monte Carlo simulations of the full evolutionary dynamics of large asexual populations, including both clonal interference and multiple-mutation effects. We consider several distributions of possible mutational effects $\rho(s)$, and determine the distribution of mutations that fix, $\rho_f(s)$, across a range of population sizes and mutation rates. We find that clonal interference analysis provides a good approximation for some aspects of $\rho_f(s)$ when large-effect mutations are sufficiently common relative to small-effect ones. When large-effect mutations are more rare, we find that an approximation focusing on multiple mutation effects, proposed by DESAI and FISHER (2007), can be more appropriate.

We next turn to the evolutionary dynamics by which beneficial mutations fix. Using our Monte Carlo approach, we simulate the dynamics of the full model with a distribution of fitness effects. We show that multiple-mutation dynamics involving mutations within a narrow range of fitness effects describes the evolution. We describe how this range of fitness effects depends on $\rho(s)$ and the other parameters, and how the mutations within this range accumulate.

MODEL AND SIMULATION METHODS

We consider an asexual population of N haploid individuals with an overall mutation rate U_b towards beneficial mutations. Our model also applies to asexual diploids, where the fitness effects of mutations refer to their effects in the individual in which they occur. Given that a beneficial mutation occurs, we assume that its fitness effect is s (i.e. the fitness of the organism increases by a factor of e^s) with probability

$$\rho(s) = \frac{e^{-(s/\sigma)^\beta}}{\sigma\Gamma(1 + 1/\beta)}, \quad (1)$$

where the two parameters σ and β characterize the shape of the distribution and Γ is the Gamma function. This form for $\rho(s)$ allows us to explore the importance of the shape of the tail of the distribution of mutant effects — that is, the relative rareness of large-effect mutations compared to small-effect ones. When $\beta = 1$, the distribution of mutant effects is exponential with mean σ . When $\beta > 1$, the distribution of mutant effects falls off faster

than exponentially (i.e. large-effect mutations are more rare), and the effect of a “typical” beneficial mutation is σ . When $\beta < 1$ the distribution of mutation effects falls off more slowly than exponentially (large-effect mutations are more common), and again the effect of a typical beneficial mutation is σ . Note that this distribution is normalized to 1, so beneficial mutations with effect between s and $s + ds$ occur at a rate $U_b \rho(s) ds$. The average fitness effect of a beneficial mutation, $\langle s \rangle$, is

$$\langle s \rangle = \sigma \frac{\Gamma(2/\beta)}{\Gamma(1/\beta)}, \quad (2)$$

so while σ is always a typical effect of a beneficial mutation, it is only exactly equal to the average effect for $\beta = 1$. We assume that there is no epistasis, so that an individual with two mutations of effect s_1 and s_2 has fitness $e^{s_1+s_2}$ (or more generally for n mutations, the fitness is $\prod_{i=1}^n e^{s_i}$). We neglect deleterious mutations, as these are not expected to qualitatively affect the dynamics in large populations when beneficial mutations are relatively common, which is the situation we study (DESAI and FISHER, 2007; ROUZINE *et al.*, 2003).

We assume a dynamics with discrete generations. In each generation, we first randomly select which individuals will survive to the next generation, weighted by each individual’s fitness. The overall survival probabilities are normalized so that on average half of the population will survive to the next generation. Each surviving individual then duplicates to create two identical individuals in the next generation. Finally, each of these individuals in the next generation has a probability U_b of acquiring a new beneficial mutation. We then repeat this algorithm for the subsequent generation. We record all the information about the genetic state of the population at each step. All simulations were checked to ensure that the results were extracted after a steady-state had been achieved. Note that this algorithm does not enforce an exact population size N at each step, but rather keeps the average population size equal to N .

These evolutionary dynamics have the advantage of being fast to simulate, allowing us to explore a greater range of parameters in a reasonable amount of computation time. However, they are slightly different from standard Wright-Fisher dynamics. It is not clear which of these models is the best representation of any particular population, but our model might be expected to correspond to a bacterial or yeast population which divides by binary fission. The differences between models do lead to small differences in establishment probabilities,

and thus are expected to cause minor modifications to the evolutionary dynamics. However, we have also simulated the standard Wright-Fisher dynamics for many of the parameters we describe in this paper, and the results are all qualitatively similar.

RESULTS

The Distribution of Mutations that Fix

We begin by studying the distribution of mutations that fix, $\rho_f(s)$, as compared to the distribution of mutations that occur, $\rho(s)$. When N and U_b are sufficiently small, neither clonal interference nor multiple mutations will occur. Thus the distribution of mutations that fix equals the distribution of mutations that establish. We expect

$$\rho_f(s) = \pi(s)\rho(s), \quad (3)$$

valid for small N and U_b , where $\pi(s)$ is the establishment probability. Note that by convention we will assume $\rho_f(s)$ is *not* normalized; this will make various calculations much more transparent. In our model, this establishment probability is given by

$$\pi(s) = \frac{1 - e^{-2s}}{1 - e^{-2Ns}}, \quad (4)$$

assuming that s is the fitness advantage relative to the background population. When $Ns \ll 1$ we have $\pi(s) \approx \frac{1}{N}$, while for $Ns \gg 1$ but $s \ll 1$ we have $\pi(s) \approx 2s$. This small-population limit of $\rho_f(s)$, which is the distribution of mutations that establish, is sometimes called the distribution of *contending* mutations (ROZEN *et al.*, 2002). We will denote it by $\rho_c(s)$.

In larger populations, we expect clonal interference to suppress the fixation of small-effect mutations. Thus for small s , we expect $\rho_f(s)$ to be smaller than $\rho_c(s)$. But clonal interference cannot suppress the fixation of the largest-effect mutations, so if it were the only important effect we would expect that for large s , $\rho_f(s)$ should equal $\rho_c(s)$. Provided that small-effect mutations are common enough relative to those of larger effect, however, multiple small- s mutations can suppress the fixation of large- s mutations. DESAI and FISHER (2007) suggest that this will occur whenever the distribution of mutation effects falls off faster than exponentially (i.e. when $\beta > 1$). When this is true, we expect that these multiple mutation

effects will cause $\rho_f(s)$ to be smaller than $\rho_c(s)$ even for large s . When $\beta \leq 1$, large-effect mutations will typically not be out-competed by multiple smaller-effect mutations, so $\rho_f(s) = \rho_c(s)$ for large s , though multiple mutations will often still be important to the dynamics of adaptation.

In Fig. 1, we show several examples of the distribution of fixed mutations $\rho_f(s)$ compared to the distribution of possible and contending mutations, $\rho(s)$ and $\rho_c(s)$ respectively. The predictions of clonal interference analysis are also shown (see Discussion). We see that the above expectations are met. For small populations (Fig. 1a), $\rho_f(s) = \rho_c(s)$ except for very small s (these s are so small that clonal interference prevents them from fixing even in these small populations). We find similar results for small populations regardless of β (data not shown). For larger populations, the behavior depends on β . In all cases, small-effect mutations are suppressed quite dramatically by clonal interference effects (Fig. 1b-d). Note, however, that clonal interference analysis predicts that this suppression of small-effect mutations should be even stronger than we observe. Presumably this is because some of these small-effect mutations are able to fix in multiple-mutation combinations together with those of larger effect. For large β , the largest-effect mutations are also suppressed, presumably by multiple-mutation effects (Fig. 1b).

Which Mutations Contribute To Adaptation

To determine how beneficial mutations of different effects contribute to the overall adaptation of the population, we need to weight mutations by their fitness effects. That is, a single fixed mutation with effect $2s$ contributes the same amount to the adaptation of the population as two mutations with effect s . Thus $R(s) \equiv s\rho_f(s)$ is the distribution of the relative contributions to the overall adaptation as a function of s . The integral of $R(s)$ from s_1 to s_2 is the total contribution of mutations of size between s_1 and s_2 to the adaptation.

Using $R(s)$, we can study which mutations are most important. We expect that mutations of very small effect will not contribute substantially to adaptation, because they are strongly suppressed by clonal interference and do not contribute much even when they do fix. On the other hand, mutations of very large effect will be too rare to contribute substantially, and may be impeded by multiple smaller mutations. Thus we expect that typically $R(s)$

will have a peak at some intermediate value of s , with some range of mutations around this that contribute substantially to adaptation. This is indeed what we find. We characterize $R(s)$ by its mean, which we call \tilde{s} . In practice, this mean is a good estimate of the “peak” of $R(s)$. We estimate the width of the range of mutations around the mean which contribute substantially to the evolution by the standard deviation of $R(s)$ around \tilde{s} , which we call $SD(s)$.

In Fig. 2, we show how \tilde{s} in our simulated populations depends on N and U_b for several different values of β . We compare these simulated results to the predictions of clonal interference analysis alone and, for $\beta > 1$, the analysis of DESAI and FISHER (2007), which combines elements of clonal interference and multiple mutations in an ad-hoc way (see Discussion).

In Fig. 3, we show $SD(s)/\tilde{s}$ as a function of N and U_b , again for several values of β , compared to the predictions of clonal interference analysis. Note that $SD(s)/\tilde{s} \ll 1$ corresponds to the case where a narrow range of mutations around \tilde{s} dominate the evolution. We see that this is typically the case, regardless of whether the distribution of mutational effects falls off faster or more slowly than exponentially, except for small N or U_b .

The Dynamics of Adaptation

We now turn to the dynamics by which these important mutations accumulate. We have seen that multiple mutations are important in determining \tilde{s} for $\beta > 1$, but not so important for $\beta \leq 1$. Despite this, mutations of effect around \tilde{s} , which dominate the overall adaptation of the population, may accumulate via multiple-mutations dynamics even when $\beta \leq 1$, although mutations of much larger effect fix whenever they establish.

These multiple-mutations dynamics are easier to understand intuitively in an idealized model where all mutations confer the *same* fitness advantage s . If this were the case, we could describe the state of the population as a distribution of the number of such mutations each individual has. Some lucky most-fit individuals have more than the average number of such mutations, and it is only additional mutations within this small subpopulation that will contribute to the long-term evolution of the population; others will eventually go extinct because they are handicapped by their relatively poor genetic background. We define the

lead, q , to be the number of such mutations the most-fit individual possesses in excess of the average individual (more precisely, $q-1$ is defined to be the difference in number of mutations between the most-fit class of established individuals and the mean individual). Several studies have analyzed the accumulation of beneficial mutations when multiple mutants are important (i.e. $q > 1$), and found that these multiple mutations dramatically affect the evolutionary dynamics (DESAI and FISHER, 2007; ROUZINE *et al.*, 2008, 2003).

When mutations have a range of fitness effects, the dynamics are clearly more complex. Yet as we have seen, mutations in some narrow range around some \tilde{s} dominate the evolution. It is therefore natural to expect that multiple mutations of effect of order \tilde{s} may routinely appear, and that their accumulation be described roughly by the single- s model, with s chosen to be \tilde{s} , and the mutation rate \tilde{U}_b the overall mutation rate to mutations within roughly $\pm SD(s)$ of \tilde{s} . We can define the lead q in this more complex situation as the fitness of the most-fit individual minus the fitness of the mean individual, divided by \tilde{s} . That is, q is the number of extra \tilde{s} -sized mutations that the most-fit individual has compared to the average individual (more precisely, we define $q-1$ as the fitness of the most-fit established class minus the average fitness, divided by \tilde{s}).

In Fig. 4, we show how this q depends on N and U_b for several different values of β . We see that even for $\beta \leq 1$, these multiple mutations are important to the dynamics (where values of $q = 3$ to 5 are reached). Note that the original clonal interference analysis implicitly assumes no multiple mutations. Thus it implies that q is between 1 and 2, depending on whether an established mutant group is sweeping to fixation.

As beneficial mutations accumulate, the population adapts. We define the rate of adaptation, v , to be the rate at which the average fitness of the population increases. In Fig. 5, we show how this v depends on N and U_b , again for several values of β . We compare these to the predictions of clonal interference theory alone and to the analysis of DESAI and FISHER (2007) (see Discussion).

DISCUSSION

Our Monte Carlo simulation approach allows us to study the evolutionary dynamics of adaptation in large asexual populations, where the effects of both clonal interference and

multiple mutations interact in a subtle way. Analytic results are difficult to obtain in this complex situation, and hence such analysis has been confined to approximations that focus primarily on one or the other effect. Using our simulations, we can assess the usefulness and generality of these methods.

In its original form, which neglects the possibility of multiple mutations, clonal interference analysis predicts the distribution of mutations that contribute to adaptation, and the dynamics by which they do so (GERRISH and LENSKI, 1998; WILKE, 2004). In this analysis the probability that a beneficial mutation fixes is the probability that it establishes and then fixes before another more-fit mutation establishes. GERRISH and LENSKI (1998) found that given that a mutation of effect s has established, the expected number of more-fit mutations establishing before the original mutation fixes is roughly

$$\lambda(s) \approx \frac{NU_b}{s} \ln N \int_s^\infty \pi(x) \rho(x) dx, \quad (5)$$

assuming that all mutations arise in the wild-type population. Thus the distribution of mutations that fix is

$$\rho_f(s) = \pi(s) e^{-\lambda(s)} \rho(s). \quad (6)$$

In Fig. 1, we compare this prediction to the results of our simulations. From Eq. (6) it is also straightforward to calculate the expected \tilde{s} and $SD(s)$. Because clonal interference becomes more likely as either population size or mutation rate increases, increasing either of these parameters is expected to increase \tilde{s} . These predictions are shown in Figs. 2 and 3.

The average rate at which mutations fix equals the rate at which those destined to fix occur. Thus clonal interference analysis predicts that the average fixation rate $\langle k \rangle$ is

$$\langle k \rangle = NU_b \int_0^\infty \rho_f(s) ds. \quad (7)$$

This means that the rate of adaptation v is

$$v = \langle k \rangle \langle s \rangle, \quad (8)$$

where $\langle s \rangle$ is the average fitness of mutations that fix. This prediction is shown in Fig. 5.

For $\beta = 0.5$ and $\beta = 1$, we see from Fig. 2 that clonal interference yields reasonable estimates of \tilde{s} . This makes sense, as in this regime multiple mutations do not suppress the fixation of larger-effect mutations. For $\beta = 10$, clonal interference systematically overestimates \tilde{s} , by an amount which increases with the population size and mutation rate. This

also makes sense, as in large populations for $\beta = 10$ multiple mutations in fact suppress the fixation of large-effect mutations.

Although clonal interference accurately predicts \tilde{s} for small β , we can see from Fig. 4 that for all values of β , q is greater than 2 when N and U_b are large, pointing to the importance of multiple mutations in the dynamics. Clonal interference analysis, by contrast, assumes that all mutations occur and fix in the wild-type population, which implies q between 1 and 2. This underlies the calculation of the fixation rate in Eq. (7), which assumes that mutations in any individual can contribute to adaptation, when in fact for $q > 1$ it is only the mutations in the relatively rare individuals that already have other beneficial mutations which contribute. Thus we expect that neglecting the importance of multiple mutations should lead clonal interference analysis to overestimate the rate of adaptation v , for all β . This is indeed what we find for $\beta = 0.5$, but we see from Fig. 5 that clonal interference analysis accurately predicts v for $\beta = 1$, and actually underestimates the rate of adaptation for $\beta = 10$.

The reason for this discrepancy is apparent from Fig. 3, which shows that for $\beta = 1$ and $\beta = 10$, clonal interference tends to underestimate $SD(s)$. This problem gets worse as N and U_b increase. The reason for this underestimate is that clonal interference assumes that the largest mutation that occurs before any other fixes goes to fixation by itself. This strongly suppresses the fixation of mutations which have a substantially smaller fitness effect, and leads to a prediction of a very small $SD(s)$. But in fact, mutations with a variety of smaller effects will sometimes happen to occur in individuals that have this larger-effect mutation, and these will sweep to fixation together. This broadens the distributions of mutations that fix, and hence increases the actual $SD(s)$, as is apparent in Fig. 3 and in the distributions shown in Figs. 1b and 1c. This means that clonal interference assumes that only mutations within a much narrower range of fitness effects contribute to adaptation than is actually the case, which should lead to underestimates of the rate of adaptation. In other words, although only mutations that happen in very fit individuals can contribute (which slows adaptation), many mutations of various effects occur in these fit individuals and can all fix together (speeding adaptation). This underestimate of v is more severe for larger β , because larger β corresponds to a larger underestimate of $SD(s)$. We see from Fig. 5 that for $\beta = 1$, this underestimate of v roughly cancels the overestimate of v caused by the assumption that

mutations in any individual can contribute to adaptation. For $\beta = 0.5$, the underestimate of $SD(s)$ is less severe, so it only partially cancels the overestimate, and in sum clonal interference overestimates the rate of adaptation. For $\beta = 10$, the reverse is true.

Together, these results suggest that clonal interference analysis is the right framework for estimating \tilde{s} whenever $\beta \leq 1$. For $\beta = 0.5$, it also gets the distribution of mutations that fix roughly correct, while for $\beta = 1$ it underestimates $SD(s)$, and hence misunderstands the distribution of mutations that actually fix. For $\beta = 10$, it does not accurately predict either \tilde{s} or the shape of the distribution of mutations that fix. Although it gives accurate estimates of v for $\beta = 1$, it is apparent that for all β clonal interference remains an incomplete picture of the dynamics; multiple mutations are also important in a variety of ways.

An alternative framework, which focuses primarily on multiple-mutation effects, was proposed by DESAI and FISHER (2007). These and other authors studied a model where all beneficial mutations have the *same* fitness advantage s (DESAI and FISHER, 2007; RIDGWAY *et al.*, 1998; ROUZINE *et al.*, 2008, 2003). They calculated the rate at which these mutations accumulate, $v(s)$, as a function of population size and mutation rate. DESAI and FISHER (2007) then argued that in a more general situation where beneficial mutations have a range of fitness effects, under many conditions $SD(s)$ should be small compared to \tilde{s} , so that mutations within a narrow range of fitness effects dominate the evolution. Thus the single- s model describes the full dynamics, provided that one chooses that single s to be \tilde{s} , and chooses the beneficial mutation rate to these mutations to be the total mutation rate towards all mutations within roughly $SD(s)$ of \tilde{s} . This should be true as long as $SD(s)$ is relatively narrow — at most of order \tilde{s} . Our simulations show that this is indeed the case (Fig. 3), as do recent experimental studies in *S. cerevisiae* and *E. coli* (DESAI *et al.*, 2007; HEGRENESS *et al.*, 2006).

Of course, the value of \tilde{s} and the width of the range of mutations which contribute to the evolution depend on $\rho(s)$, N , and the overall mutation rate. A full understanding of this depends in a subtle way on both clonal interference and multiple-mutation effects, but DESAI and FISHER (2007) proposed a simple approximation. They first calculate $v(s)$ for each possible value of s , assuming that only mutations of this size are possible. To do this, one must specify an appropriate mutation rate to mutations of this size, which we refer to as \tilde{U}_b . DESAI and FISHER (2007) made the ad-hoc assumption that this mutation rate should

be the total mutation rate to mutations of order s (i.e. within roughly a factor of 2 of s). They then calculated $v(s)$. This $v(s)$ expresses the contribution of mutations of effect s to the overall evolution, and thus should equal $R(s)$, up to normalization. From this $R(s)$, they calculate \tilde{s} . They find

$$\tilde{s} = \sigma \left[\frac{\ell}{\beta - 1} \right]^{1/\beta}, \quad (9)$$

where ℓ is related to the overall mutation rate by

$$\ell = -\ln \left[\frac{U_b}{\sigma \Gamma(1 + 1/\beta)} \right]. \quad (10)$$

This expression for \tilde{s} is only valid for $\beta > 1$; for distributions of mutational effects that fall off exponentially or slower the behavior is more complicated and the analysis breaks down.

Both this approximation and the original clonal interference analysis predict that \tilde{s} should increase with N , because increasing the population size increases the probability of clonal interference but does not dramatically change the relative importance of large effect mutations relative to multiple smaller-effect ones. On the other hand, for large β , multiple-mutation effects should cause a qualitative shift in the relationship between \tilde{s} and U_b . Clonal interference analysis alone predicts that \tilde{s} increases with U_b , because higher mutation rates make clonal interference more common. However, higher mutation rates also increase the importance of multiple small-effect mutations relative to large-effect ones. From Eq. (9) we see that for $\beta > 1$ this should mean that \tilde{s} actually *decreases* with U_b for large U_b . Although the effect is small, we do observe this decrease in our simulations (Fig. 2a). For small β , on the other hand, we expect that multiple mutation effects typically do not impede the fixation of large-effect mutations. Thus clonal interference alone gives a qualitatively accurate picture of how \tilde{s} depends on N and U_b , as observed.

Given \tilde{s} , and assuming that the appropriate mutation rate is that towards mutations of this order, the dynamics of adaptation are similar to that of the corresponding single- s model. Using Eq. (9) and their analysis of the single- s model, DESAI and FISHER (2007) calculated how the rate of adaptation v and the lead q should depend on N and U_b and the shape of the distribution of mutational effects. They found

$$q \approx \frac{2 \ln [N\sigma] (\beta - 1)}{\ell \beta}, \quad (11)$$

and

$$v \approx 2C_\beta \sigma^2 \frac{\ln[N\sigma]}{\ell^{2-2/\beta}}, \quad \text{where} \quad C_\beta \equiv \frac{(\beta-1)^{2-2/\beta}}{\beta^2}. \quad (12)$$

As with Eq. (9), these expressions are only valid for $\beta > 1$.

We compare these theoretical predictions to our simulation results in Figs. 2, 3 and 5. We see that for large N and U_b they give qualitatively the correct behavior for \tilde{s} , the lead q , and the rate of adaptation v , though they do systematically overestimate q and v (see below). In this regime, these results are more accurate than those given by clonal interference analysis. Two qualitative features are particularly important: that q can become larger than 2, and that \tilde{s} actually *decreases* as U_b increases when $\beta > 1$. For small N and U_b , corresponding to $q \leq 2$, the multiple-mutations results are less accurate, as expected because the above results are valid only when $q \gtrsim 2$ (DESAI and FISHER, 2007).

Eq. (11) and Eq. (12) rely on the ad-hoc assumption that the appropriate mutation rate to the mutations around \tilde{s} that dominate the dynamics is the total mutation rate to mutations of order \tilde{s} (i.e. within roughly a factor of 2 of \tilde{s}). As we have found here, $SD(s)$ is often much smaller than \tilde{s} , so the range of mutational effects that contributes substantially to the evolution is much smaller than assumed. This means that the intuitive picture behind the multiple-mutations model of the dynamics is correct: there is indeed a narrow range of mutations which contribute to the evolution, and their accumulation is well-described by a corresponding single- s model of the dynamics. However, the estimate of the appropriate mutation rate is too large, since a narrower range contributes than was assumed. This means that the predictions of q and v in Eq. (11) and Eq. (12) should be overestimates, as we observe. To correct these overestimates, we need to understand what determines $SD(s)$. Unfortunately neither clonal interference analysis nor the multiple-mutations approach does this well; it remains an important topic for future analytical work.

While the clonal interference and the multiple-mutations approximations together help us to form a more complete understanding of the dynamics, both leave much to be desired. Clonal interference processes appear to be the main determinant of \tilde{s} when $\beta \leq 1$, as demonstrated by Fig. 2. But even for these small β , we see that q is often larger than 2, and hence clonal interference analysis gives the wrong picture for the dynamics. Further, it misses the possibility of smaller-effect mutations fixing together with those of effect roughly \tilde{s} , and hence drastically underestimates $SD(s)$ even for $\beta = 1$. On the other hand, while

the multiple-mutations analysis provides the right picture of the dynamics for $\beta > 1$, and accurately predicts \tilde{s} , q and v , it provides no way to estimate $SD(s)$, nor any specific predictions when $\beta \leq 1$. The simulation approach we have taken in this paper sheds some light on where and why these two different approaches work, and has highlighted the regimes where neither provides a satisfactory picture. A more detailed understanding will require analysis of a general model which explicitly incorporates both clonal interference and multiple mutations, to produce a theory which has the correct picture of the dynamics in these difficult regimes.

An interesting result of our simulations is that the general shape of the distribution of the mutations that contribute to adaptation, $R(s)$, is rather universal. $R(s)$ is always a relatively narrow distribution with a clear peak at some \tilde{s} . The distribution of mutations that fix, $\rho_f(s)$, has a similar shape with a sharp peak near \tilde{s} . This means that if we do a single experiment at a given population size and mutation rate, the observed $\rho_f(s)$ will not provide much information about the underlying $\rho(s)$. This lack of sensitivity of experimental adaptation to the distribution of mutational effects has been noted in a related context by HEGRENESS *et al.* (2006). However, our simulations also show that the scaling of various aspects of $\rho_f(s)$ (such as \tilde{s}) with population size and mutation rate *does* depend strongly on $\rho(s)$. Most important is the shape of the tail of $\rho(s)$; as we have seen, the way in which \tilde{s} depends on N and U_b is strongly dependent on β . Thus careful experiments which are carried out at a range of population sizes or mutation rates may make it possible to infer important aspects of $\rho(s)$ from measurements of $\rho_f(s)$ or the rate of adaptation v .

As our simulations make clear, the actual values of β applicable to natural asexual populations are of central importance to the dynamics by which these populations adapt. The values of β found in natural populations may also tell us something about the evolutionary history of these populations. Orr and Gillespie have argued that if an individual is at a random high-fitness genotype, the distribution of more-fit genotypes is exponential, so we should expect $\beta = 1$ (GILLESPIE, 1983, 1984, 1991; ORR, 2002, 2003). However, as a population adapts it is natural to expect $\rho(s)$ to change. For example, a population may face a static challenge, and gradually deplete the available beneficial mutations as it adapts. If the population were small enough that $\rho_f(s) = 2s\rho(s)$, the distribution $\rho(s)$ should converge to an exponential as this adaptation progresses. But if clonal interference and multiple-

mutation effects cause large-effect mutations to be depleted much faster than small-effect ones, we expect that β should increase as the available mutations become depleted. Thus large observed values of β may be indicative of this type of adaptation. Of course, this increase in β could be avoided if the accumulation of beneficial mutations tends to open up new possibilities for further adaptation. In other words, the structure of fitness landscapes has an important role in determining typical values of β , and how these change as populations adapt. Given these values of β , our simulations provide a way to understand, in a statistical sense, which mutations will tend to contribute to adaptation, and the dynamics by which they will do so.

ACKNOWLEDGMENTS

JLN and CF acknowledge support from the University of Colorado and the Undergraduate Research Opportunity Program at the University of Colorado. MMD acknowledges support from Center grant P50GM071508 from the National Institute of General Medical Science to the Lewis-Sigler Institute.

Literature Cited

- DE VISSER, J., C. W. ZEYL, P. J. GERRISH, J. L. BLANCHARD, and R. E. LENSKE, 1999 Diminishing returns from mutation supply rate in asexual populations. *Science* **283**: 404–406.
- DE VISSER, J. A. G. M. and D. E. ROZEN, 2005 Limits to adaptation in asexual populations. *Journal of Evolutionary Biology* **18**: 779–788.
- DEPRISTO, M. A., D. M. WEINREICH, and D. HARTL, 2005 Missense meanderings in sequence space: A biophysical view of protein evolution. *Nature Reviews Genetics* **6**: 678–687.
- DESAI, M. M. and D. S. FISHER, 2007 Beneficial mutation-selection balance and the effect of linkage on positive selection. *Genetics* **176**: 1759–1798.
- DESAI, M. M., D. S. FISHER, and A. W. MURRAY, 2007 The speed of evolution and maintenance of variation in asexual populations. *Current Biology* **17**: 385–394.
- GERRISH, P., 2001 The rhythm of microbial adaptation. *Nature* **413**: 299–302.
- GERRISH, P. and R. LENSKE, 1998 The fate of competing beneficial mutations in an asexual population. *Genetica* pp. 127–144.
- GILLESPIE, J. H., 1983 A simple stochastic gene substitution model. *Theoretical Population Biology* **23**: 202–215.
- GILLESPIE, J. H., 1984 Molecular evolution over the mutational landscape. *Evolution* **38**: 1116–1129.
- GILLESPIE, J. H., 1991 *The Causes of Molecular Evolution*. Oxford University Press, Oxford.
- HALDANE, J. B. S., 1927 The mathematical theory of natural and artificial selection, part v: Selection and mutation. *Proceedings of the Cambridge Philosophical Society* **23**: 838–844.
- HEGRENESS, M., N. SHORESH, D. HARTL, and R. KISHONY, 2006 An equivalence principle for the incorporation of favorable mutations in asexual populations. *Science* **311**: 1615–1617.
- HILL, W. G. and A. ROBERTSON, 1966 Effect of linkage on limits to artificial selection. *Genetical Research* **8**: 269–294.
- IMHOF, M. and C. SCHLOTTERER, 2001 Fitness effects of advantageous mutations in evolving *Escherichia coli* populations. *PNAS* **98**: 1113–1117.

- KASSEN, R. and T. BATAILLON, 2006 Distribution of fitness effects among beneficial mutations before selection in experimental populations of bacteria. *Nature Genetics* **38**: 484–488.
- KIM, Y. and H. A. ORR, 2005 Adaptation in sexuals vs. asexuals: clonal interference and the fisher-muller model. *Genetics* **171**: 1377–1386.
- LUNZER, M., S. P. MILLER, R. FELSHEIM, and A. M. DEAN, 2005 The biochemical architecture of an ancient adaptive landscape. *Science* **310**: 499–501.
- ORR, H. A., 2002 The population genetics of adaptation: The adaptation of dna sequences. *Evolution* **56**: 1317–1330.
- ORR, H. A., 2003 The distribution of fitness effects among beneficial mutations. *Genetics* **163**: 1519–1526.
- RIDGWAY, D., H. LEVINE, and D. KESSLER, 1998 Evolution on a smooth landscape: the role of bias. *Journal of Statistical Physics* **90**: 191.
- ROKYTA, D. R., P. JOYCE, S. B. CAUDLE, and H. A. WICHMAN, 2005 An empirical test of the mutational landscape model of adaptation using a single-stranded dna virus. *Nature Genetics* **37**: 441–444.
- ROUZINE, I., E. BRUNET, and C. O. WILKE, 2008 The traveling-wave approach to asexual evolution: Muller’s ratchet and speed of adaptation. *Theoretical Population Biology* **in press**.
- ROUZINE, I., J. WAKELEY, and J. M. COFFIN, 2003 The solitary wave of asexual evolution. *PNAS* **100**: 587–592.
- ROZEN, D. E., J. DE VISSER, and P. J. GERRISH, 2002 Fitness effects of fixed beneficial mutations in microbial populations. *Current Biology* **12**: 1040–1045.
- SANJUAN, R., A. MOYA, and S. F. ELENA, 2004 The distribution of fitness effects caused by single-nucleotide substitutions in an rna virus. *Proceedings of the National Academy of Sciences of the United States of America* **101**: 8396–8401.
- WILKE, C. O., 2004 The speed of adaptation in large asexual populations. *Genetics* **167**: 2045–2053.

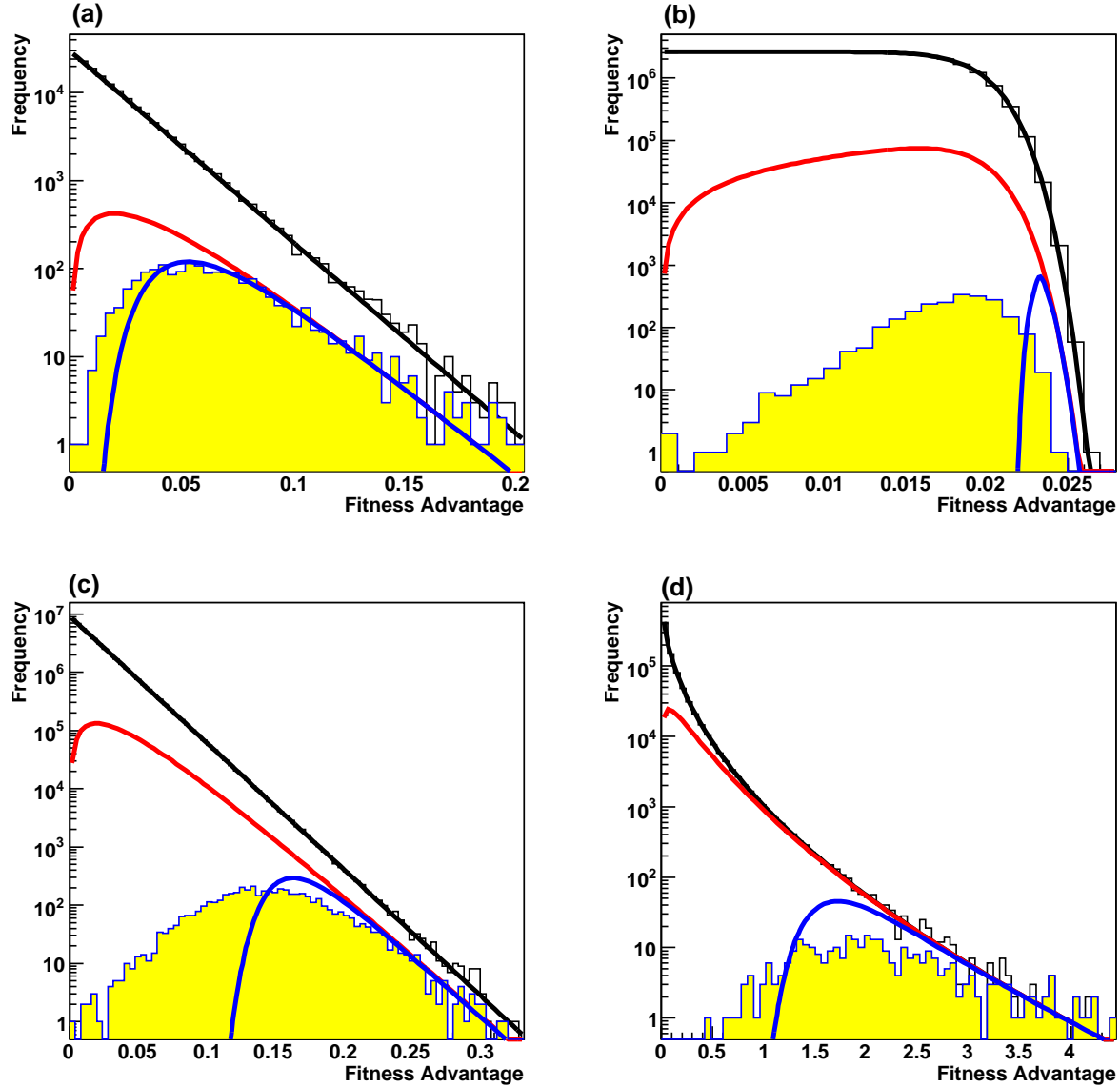


FIG. 1 Examples of the distribution of possible mutations $\rho(s)$ (solid black line), the distribution of contending mutations $\rho_c(s)$ (solid red line), and the distribution of fixed mutations $\rho_f(s)$ from our simulations (yellow histogram). Also shown is the distribution of mutations which occurred in the simulations (transparent histogram). Additionally the distribution of predicted fixed mutations $\rho_f(s)$ from a clonal interference calculation are shown (solid blue line). Note the logarithmic scale. In all examples, $\sigma = 0.02$. (a) A small population, where $\rho_f(s) = \rho_c(s)$ except for the smallest-effect mutations. Here $N = 3 \times 10^4$, $U_b = 10^{-5}$, and $\beta = 1.0$. (b) A large population with $\beta = 10$. Here $N = 10^7$ and $U_b = 10^{-5}$. Note that small-effect mutations are suppressed by clonal interference effects, while large-effect mutations are suppressed by multiple mutation effects. (c) A large population with $\beta = 1$. Here $N = 10^7$ and $U_b = 10^{-5}$. Note that small-effect mutations are suppressed by clonal interference effects, but less strongly than clonal interference analysis alone predicts. (d) A large population with $\beta = 0.5$. Here $N = 1 \times 10^7$ and $U_b = 10^{-5}$.

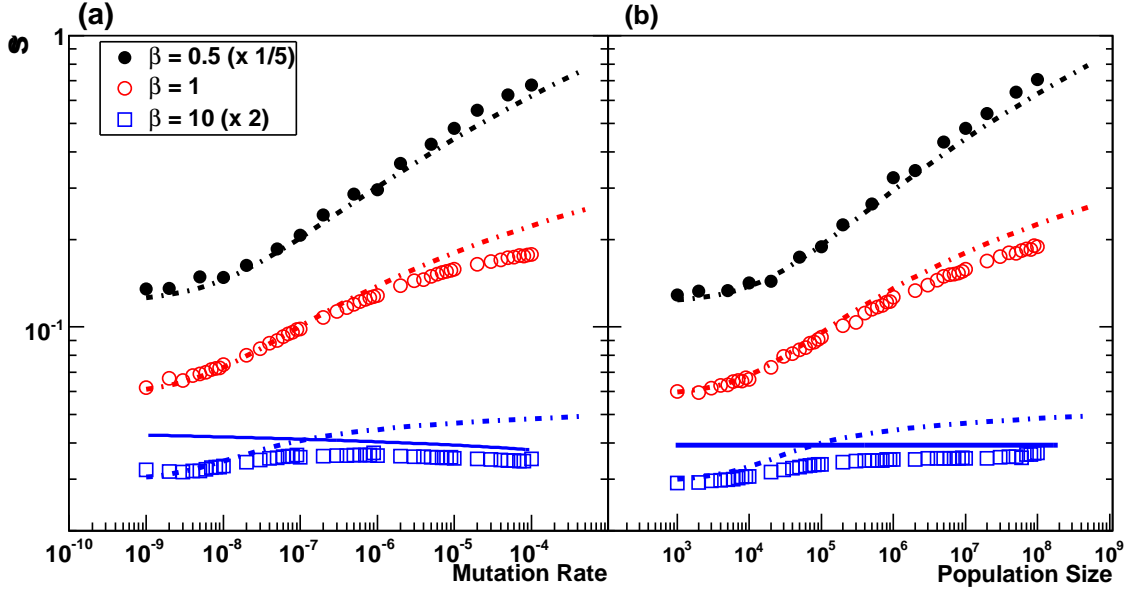


FIG. 2 The average scaled fitness effect of mutations that fix, \tilde{s} . In all cases $\sigma = 0.02$. (a) Simulation results for \tilde{s} for $N = 10^7$ as a function of U_b for $\beta = 0.5$ (closed black circles), $\beta = 1$ (open red circles), and $\beta = 10$ (open blue squares). Predictions of clonal interference analysis are shown as dotted lines, and the predictions of the multiple mutation analysis (for $\beta = 10$) are shown as a solid line. Note that for $\beta = 10$, \tilde{s} decreases with U_b for large U_b . (b) Simulation results for \tilde{s} for $U_b = 10^{-5}$ as a function of N for $\beta = 0.5$ (closed black circles), $\beta = 1$ (open red circles), and $\beta = 10$ (open blue squares). Predictions of clonal interference analysis are shown as dotted lines, and the predictions of the multiple mutation analysis (for $\beta = 10$) are shown as a solid line.

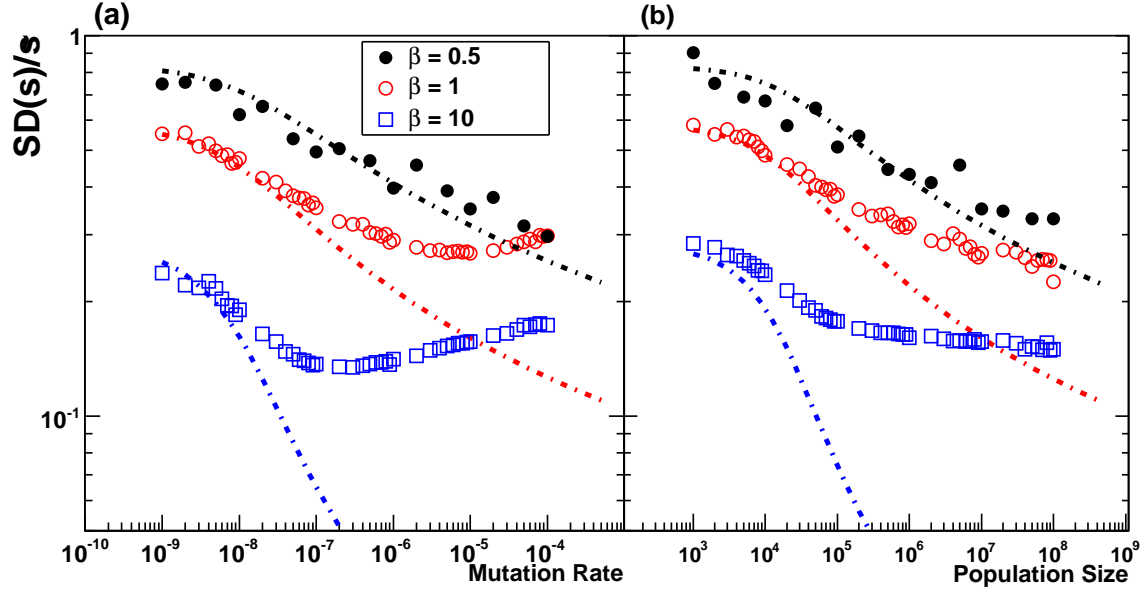


FIG. 3 The scaled width of the weighted distribution of mutations that fix, $SD(s)/\tilde{s}$. In all cases $\sigma = 0.02$. (a) Simulation results for $SD(s)/\tilde{s}$ for $N = 10^7$ as a function of U_b for $\beta = 0.5$, $\beta = 1$, and $\beta = 10$. Predictions of clonal interference analysis are shown as dotted lines. (b) Simulation results for \tilde{s} for $U_b = 10^{-5}$ as a function of N for $\beta = 0.5$, $\beta = 1$, and $\beta = 10$. Predictions of clonal interference analysis are shown as dotted lines.

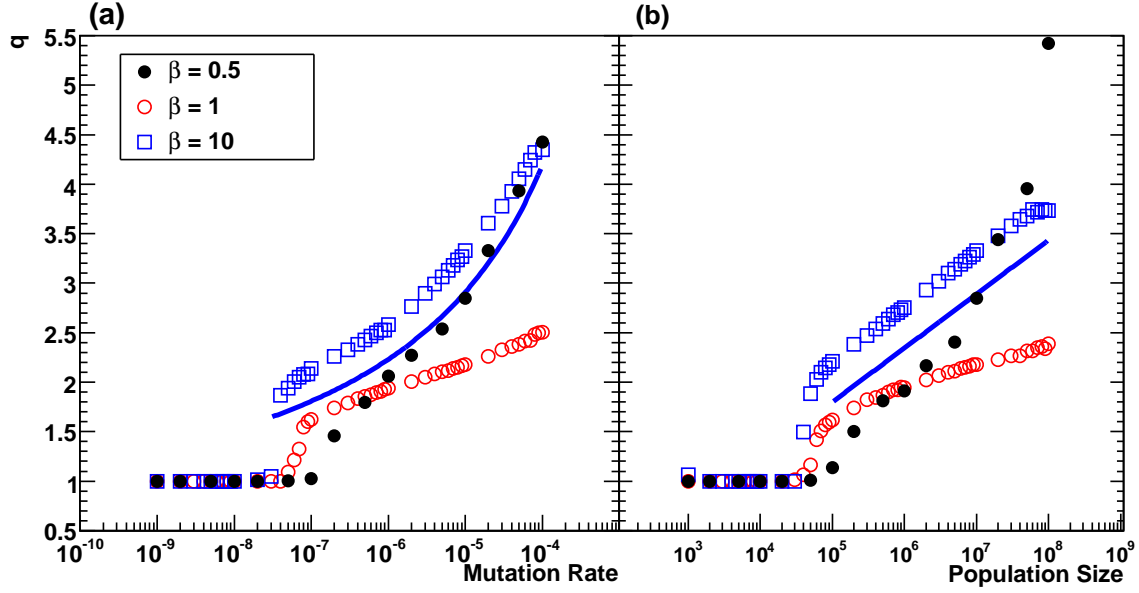


FIG. 4 The effective lead q . (a) Simulation results for q as a function of U_b for $\beta = 0.5$, $\beta = 1$, and $\beta = 10$. Other parameters are as in Fig. 3a. Predictions of the multiple-mutations analysis (for $\beta = 10$) are shown as a solid blue line. Note that clonal interference predicts $q \approx 1$, independent of the parameters. (b) Simulation results for q as a function of N for $\beta = 0.5$, $\beta = 1$, and $\beta = 10$. Other parameters are as in Fig. 3b. Predictions of the multiple-mutations analysis (for $\beta = 10$) are shown as a solid blue line. As before, clonal interference predicts $q \approx 1$, independent of the parameters.

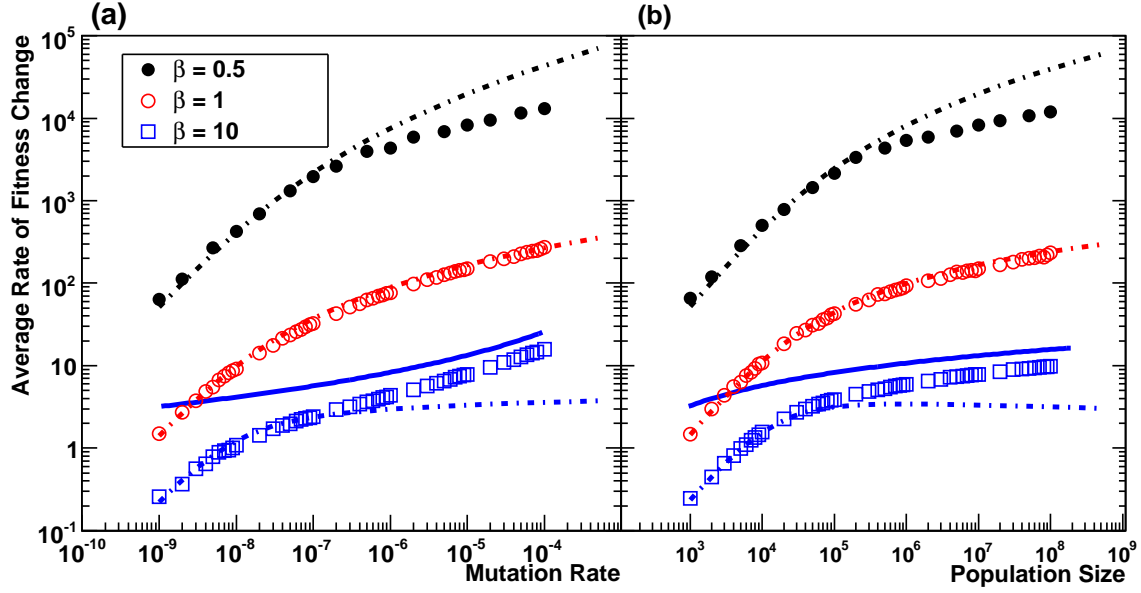


FIG. 5 The average rate of adaptation, v . (a) Simulation results for v as a function of U_b for $\beta = 0.5$, $\beta = 1$, and $\beta = 10$. Other parameters are as in Fig. 3a. Predictions of clonal interference analysis are shown as dotted lines, and the predictions of the multiple-mutations analysis (for $\beta = 10$) are shown as a solid blue line. (b) Simulation results for v as a function of N for $\beta = 0.5$, $\beta = 1$, and $\beta = 10$. Other parameters are as in Fig. 3b. Predictions of clonal interference analysis are shown as dotted lines, and the predictions of the multiple-mutations analysis (for $\beta = 10$) are shown as a solid blue line.